J|A|C|S
ARTICLES

Published on Web 07/23/2010

Conformations, Conformational Preferences, and Conformational Exchange of N′-Substituted *N*-Acylguanidines: Intermolecular Interactions Hold the Key

Roland Kleinmaier,[‡] Max Keller,[†] Patrick Igel,[†] Armin Buschauer,[†] and Ruth M. Gschwind*[,‡]

Institut für Organische Chemie and Institut für Pharmazie, Universität Regensburg, Universitätsstrasse 31, D-93053 Regensburg, Germany

Received May 3, 2010; E-mail: ruth.gschwind@chemie.uni-regensburg.de

Abstract: Guanidine and acylguanidine groups are crucial structural features of numerous biologically active compounds. Depending on the biological target, acylguanidines may be considered as considerably less basic bioisosteres of guanidines with improved pharmacokinetics and pharmacodynamics, as recently reported for N′-monoalkylated *N*-acylguanidines as ligands of G-protein-coupled receptors (GPCRs). The molecular basis for enhanced ligand−receptor interactions of acylguanidines is far from being understood. So far, only a few and contradictory results about their conformational preferences have been reported. In this study, the conformations, conformational preferences, and conformational exchange of four unprotonated and seven protonated monoalkylated acylguanidines with up to six anions and with bisphosphonate tweezers are investigated by NMR. Furthermore, the effects of the acceptor properties in acylguanidine salts, of microsolvation by dimethylsulfoxide, and of varying acyl and alkyl substituents are studied. Throughout the whole study, exclusively two out of eight possible acylguanidine conformations were detected, independent of the compound, the anion, or the solvent used. For the first time, it is shown that the strength and number of intermolecular interactions with anions, solvent molecules, or biomimetic receptors decide the conformational preferences and exchange rates. One recently presented and two new crystal structures resemble the conformational preferences observed in solution. Thus, consistent conformational trends are found throughout the structurally diverse compound pool, including two potent GPCR ligands, different anions, and receptors. The presented results may contribute to a better understanding of the mechanism of action at the molecular level and to the prediction and rational design of these biologically active compounds.

Introduction

Guanidine compounds are highly valued in various biological, biochemical, and medical applications,[1−3] including inhibition of enzymes[4] and the Na^+-H^+ ion exchanger (NHE),[5,6] as substances with positive inotropic effects,[7] as anticoagulants,[8] and as highly active ligands of transmembrane receptors from various families, e.g., aminergic and peptidergic G-protein-coupled receptors (GPCRs) such as histamine and neuropeptide Y receptors.[9−11] Especially in the field of medicinal chemistry, acylguanidines are greatly appreciated because they show improved pharmacokinetic properties compared to those of the corresponding guanidines, while retaining or even improving the biological activity.[9−11] Acylation of guanidine reduces its basicity by 4−5 orders of magnitude, which improves the pharmacokinetic properties, but retains its general ability to interact with acidic functions of the biological target.[9] Indeed, the increased acidity of the acylguanidinium NH protons leads to stronger binding to carboxylates compared to that observed for simple guanidinium cations,[12] e.g., in supramolecular assemblies.[13]

[‡] Institut für Organische Chemie.
[†] Institut für Pharmazie.

(1) Katritzky, A. R.; Rogovoy, B. V.; Cai, X.; Kirichenko, N.; Kovalenko, K. V. *J. Org. Chem.* **2004**, *69*, 309–313.
(2) Saczewski, F.; Balewski, Ł. *Exp. Opin. Ther. Patents* **2009**, *19*, 1417–1448.
(3) Berlinck, R. G. S.; Burtoloso, A. C. B.; Kossuga, M. H. *Nat. Prod. Rep.* **2008**, *25*, 919–954.
(4) Cole, J.; et al. *Bioorg. Med. Chem. Lett.* **2008**, *18*, 1063–1066.
(5) Lee, S.; Kim, T.; Lee, B. H.; Yoo, S.; Lee, K.; Yi, K. Y. *Bioorg. Med. Chem. Lett.* **2007**, *17*, 1291–1295.
(6) Baumgarth, M.; Beier, N.; Gericke, R. *J. Med. Chem.* **1997**, *40*, 2017–2034.
(7) Buschauer, A. *J. Med. Chem.* **1989**, *32*, 1963–1970.
(8) O'Connor, S. P.; Atwal, K.; Li, C.; Liu, E. C.-K.; Seiler, S. M.; Shi, M.; Shi, Y.; Stein, P. D.; Wang, Y. *Bioorg. Med. Chem. Lett.* **2008**, *18*, 4696–4699.
(9) Ghorai, P.; Kraus, A.; Keller, M.; Goette, C.; Igel, P.; Schneider, E.; Schnell, D.; Bernhardt, G.; Dove, S.; Zabel, M.; Elz, S.; Seifert, R.; Buschauer, A. *J. Med. Chem.* **2008**, *51*, 7193–7204.
(10) Schneider, E.; Keller, M.; Brennauer, A.; Hoefelschweiger, B. K.; Gross, D.; Wolfbeis, O. S.; Bernhardt, G.; Buschauer, A. *ChemBioChem* **2007**, *8*, 1981–1988.
(11) Brennauer, A.; Dove, S.; Buschauer, A. Neuropeptide Y and related peptides. In *Handbook of Experimental Pharmacology*; Michel, M. C., Ed.; Springer: Berlin/Heidelberg, 2004; Vol. 162, pp 505−546.
(12) Schug, K. A.; Lindner, W. *Chem. Rev.* **2005**, *105*, 67–113.
(13) Schlund, S.; Schmuck, C.; Engels, B. *J. Am. Chem. Soc.* **2005**, *127*, 11115–11124.

Regarding structural and conformational investigations of acylguanidines, extensive theoretical studies on the potassium-sparing monoacylguanidine diuretic amiloride and its derivatives in the solid state and in solution have been published.[14−17] In addition, the crystal structure of a protein−amiloride complex proved the formation of charge-assisted H-bonds between the planar acylguanidine moiety and an aspartate side chain,[18,19] which are much stronger than H-bonds between neutral species.[20,21] These charge-assisted H-bonds are similar to the famous arginine−carboxylate salt bridges,[22,23] which are crucial to the tertiary structure of many proteins[24] and have been subject of numerous theoretical studies, too.[13,24−26] For N-alkylated acylguanidines, a conformational study of rotationally restricted, i.e., mostly cyclized, acylguanidine compounds is available,[27,28] but it is limited to compounds which are at least N′,N″-bisalkylated. No compounds are included with a free NH_2 group as observed in the biologically active compounds cited above.[9−11] However, to our knowledge, for the class of N′-monosubstituted *N*-acylguanidines (further on referred to as monoalkylated acylguanidines, see Figure 1), conformational studies are still missing.

In principle, the acylguanidine moiety of both protonated and uncharged monoalkylated acylguanidines can adopt eight planar conformations. Five of these conformations are energetically unfavorable due to severe steric hindrance and/or the lack of an intramolecular H-bond (see Supporting Information for details). Each of the remaining three conformations (see Figure 1) shows an intramolecular H-bond and similar contributions to steric hindrance, suggesting small energy differences between the conformations I, II, and III or I^+, II^+, and III^+.

The main difference of conformation I/I^+ compared to conformations II/II^+ and III/III^+ is the formation of the intramolecular H-bond to the RNH or the NH_2 group, respectively. In complexes of non-acylated arginines with bisphosphonate tweezers, energetic preferences were calculated for intermolecular H-bonds to the RNH group in quantum chemical calculations[29] and molecular dynamics simulations.[30] Thus, also

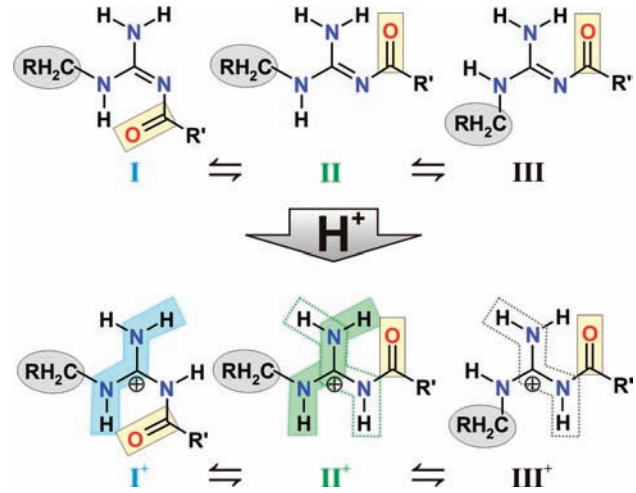

Figure 1. Possible conformations of monoalkylated acylguanidines with intramolecular H-bonds in the unprotonated (I−III) and protonated states (I^+−III^+). Zigzag pathways leading to $^4J_{H,H}$ scalar couplings between H-atoms are indicated for the protonated forms.

in acylguanidines, a preferred formation of H-bonds to the NH group might be expected (conformation I/I^+). Indeed, the only crystal structure of a monoalkylated acylguanidine published so far, to our knowledge, which is the precursor of a histamine H_2 receptor ligand crystallized as free base, shows conformation I with an intramolecular H-bond to the NH group (see Figure 2a).[9,31]

In contrast, the only existing NMR study about the H-bond pattern of an acylguanidine moiety, which was performed on a complex of an arginine derivative with bisphosphonate tweezers, reports the existence of conformation II^+ in this bioorganic model complex in solution (see Figure 2b).[32] Also a docking study of an acylguanidine-type agonist in the binding pocket of the guinea pig H_2 receptor suggests conformation II^+ (see Figure 2c).[9] Interestingly, the structure used in this docking study is a detritylated and protonated form of a close analogue of the ligand, the precursor of which adopts conformation I in the solid state, as mentioned above (Figure 2a).

The deviations among these results from theoretical calculations and NMR, X-ray, and docking studies show that monoalkylated acylguanidines may not have one generally preferred conformation but suggest that the substituents and the protonation state of the acylguanidine and/or the geometry and the H-bond acceptor qualities of the receptor may substantially influence the conformational preferences. Considering the general importance of pre-organization effects for the binding constants of complexes,[33] e.g., via H-bonding,[34] and the recent theoretical results about facilitated self-assembly of rigidified guanidines,[35] the elucidation and prediction of the conforma-

(14) Noel, J.; Germain, D.; Vadnais, J. *Biochemistry* **2003**, *42*, 15361–15368.
(15) Pretscher, A.; Brisander, M.; Bauer-Brandl, A. a.; Hansen, L. K. *Acta Crystallogr.* **2001**, *C57*, 1217–1219.
(16) Buono, R. A.; Venanzi, T. J.; Zauhar, R. J.; Luzhkov, V. B.; Venanzi, C. A. *J. Am. Chem. Soc.* **1994**, *116*, 1502–1513.
(17) Smith, R. L.; Cochran, D. W.; Gund, P.; Cragoe, E. J., Jr. *J. Am. Chem. Soc.* **1979**, *101*, 191–201.
(18) Zeslawska, E.; Schweinitz, A.; Karcher, A.; Sondermann, P.; Sperl, S.; Stuerzebecher, J.; Jacob, U. *J. Mol. Biol.* **2000**, *301*, 465–475.
(19) Zeslawska, E.; Oleksyn, B.; Stadnicka, K. *Struct. Chem.* **2004**, *15*, 567–572.
(20) Schmuck, C.; Wienand, W. *J. Am. Chem. Soc.* **2003**, *125*, 452–459.
(21) Steiner, T. *Angew. Chem.* **2002**, *114*, 50–80.
(22) Schlereth, K.; Beinoraviciute-Kellner, R.; Zeitlinger, M. K.; Bretz, A. C.; Sauer, M.; Charles, J. P.; Vogiatzi, F.; Leich, E.; Samans, B.; Eilers, M.; Kisker, C.; Rosenwald, A.; Stiewe, T. *Mol. Cell* **2010**, *38*, 356–368.
(23) Dehner, A.; Klein, C.; Hansen, S.; Müller, L.; Buchner, J.; Schwaiger, M.; Kessler, H. *Angew. Chem., Int. Ed.* **2005**, *44*, 5247–5251.
(24) Melo, A.; Ramosa, M. J.; Floriano, W. B.; Gomes, J. A. N. F.; Leao, J. F. R.; Magalhaes, A. L.; Maigret, B.; Nascimento, M. C.; Reuter, N. *J. Mol. Struct. (Theochem)* **1999**, *463*, 81–90.
(25) Condic-Jurkic, K.; Perchyonok, V. T.; Zipse, H.; Smith, D. M. *J. Comput. Chem.* **2008**, *29*, 2425–2433.
(26) Zheng, Y.-J.; Ornstein, R. L. *J. Am. Chem. Soc.* **1996**, *118*, 11237–11243.
(27) Greenhill, J. V.; lsmail, M. J.; Bedford, G. R.; Edwards, P. N.; Taylor, P. J. *J. Chem. Soc., Perkin Trans. 2* **1985**, 1265–1274.
(28) Greenhill, J. V.; lsmail, M. J.; Bedford, G. R.; Edwards, P. N.; Taylor, P. J. *J. Chem. Soc., Perkin Trans. 2* **1985**, 1255–1264.
(29) Kirchner, B.; Reiher, M. *J. Am. Chem. Soc.* **2005**, *127*, 8748–8756.
(30) Gschwind, R. M.; Armbrüster, M.; Zubrzycki, I. Z. *J. Am. Chem. Soc.* **2004**, *126*, 10228–10229.
(31) CCDC 686506 contains the supplementary crystallographic data for the compound shown in Figure 2 (available free of charge from the Cambridge Crystallographic Data Centre viawww.ccdc.cam.ac.uk/data_request/cif).
(32) Federwisch, G.; Kleinmaier, R.; Drettwan, D.; Gschwind, R. M. *J. Am. Chem. Soc.* **2008**, *130*, 16846–16847.
(33) Hettche, F.; Rei, P.; Hoffmann, R. W. *Chem.—Eur. J.* **2002**, *8*, 4946–4956.
(34) Alvarez, J.; Wang, Y.; Gomez-Kaifer, M.; Kaifer, A. E. *Chem. Commun.* **1998**, 1455–1457.
(35) Schlund, S.; Schmuck, C.; Engels, B. *Chem.—Eur. J.* **2007**, *13*, 6644–6653.

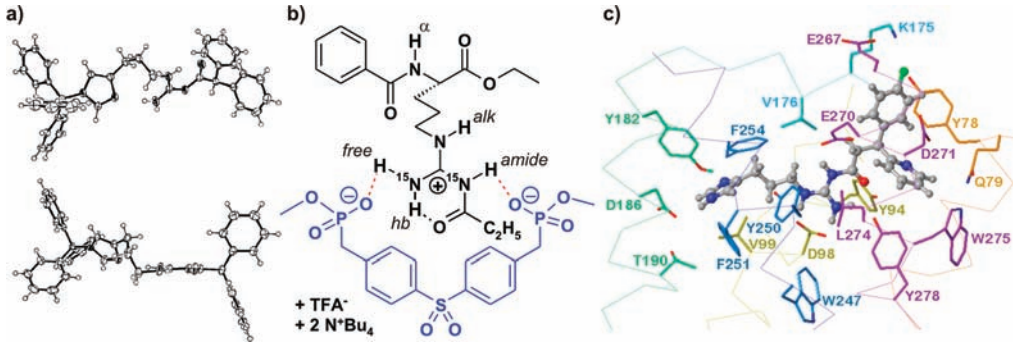

Figure 2. (a) Crystal structure representation[9,31] (ORTEP diagram) of the free base of trityl-protected acylguanidine in conformation I. (b) Bioorganic model complex of [$^{15}N^{\eta}_2$]-Bz-Arg-(N$^{\eta}$-propionyl)-OEt (conformation II$^+$) with bisphosphonate tweezers.[32] (c) Computational docking model[9] of the gpH$_2$R binding site for protonated *N*-acyl-*N*′-imidazolylpropylguanidine with H-bond, indicating conformation II$^+$.

tional preferences of monoalkylated acylguanidines may considerably support the rational development of this pharmacologically important class of ligands.

Therefore, in this study, the conformations, conformational preferences, and conformational exchange of four unprotonated and seven protonated monoalkylated acylguanidines with up to six anions and with bisphosphonate tweezers are investigated by NMR. The effect of the acceptor properties in acylguanidine salts, the influence of microsolvation by dimethylsulfoxide (DMSO), and the contribution of varying acyl and alkyl substituents to the conformational equilibria and their exchange rates are presented. Consistent conformational trends are derived depending on the strengths of the intermolecular interactions, which are additionally corroborated by two new crystal structures.

Results and Discussion

Compound Pool. For this conformational study of acylguanidines, seven model compounds were selected (Figure 3). First, [$^{15}N^{\eta}_2$]-Bz-Arg-(N$^{\eta}$-propionyl)-OEt (**1**), the acylguanidine used in the previous NMR complexation study, was chosen to enable a comparison between the acylguanidine conformations in the free state and bound to an artificial receptor molecule.[32] Second, two highly potent acylguanidine-type GPCR ligands were investigated, the histamine H_4 receptor agonist UR-PI294[36] (**2**) and the arginine-derived neuropeptide Y (NPY) Y_1 receptor selective antagonist UR-MK50 (**3**), which is an acylated derivative of the first potent and selective Y_1 receptor antagonist, BIBP 3226.[37] Third, *N*-propionyl-*N*′-butylguanidine (**4a**) and *N*-cinnamoyl-*N*′-butylguanidine (**4b**) were chosen as acylguanidines with very simple alkyl substituents and strongly differing acyl substituents to eliminate any interference from additional functional groups in the alkyl moiety. Finally, to further investigate the influence of structural and electronic variations in the acyl substituents, the para-substituted benzoic acid derivatives *N*-*p*-dimethylaminobenzoyl-*N*′-butylguanidine (**4c**) and *N*-*p*-methoxybenzoyl-*N*′-butylguanidine (**4d**) were used.

The syntheses of **1**[38] and **2**[36] have already been reported, while the syntheses of **3** and **4a**−**d** are described in the Experimental Section, and further details can be found in the Supporting Information.

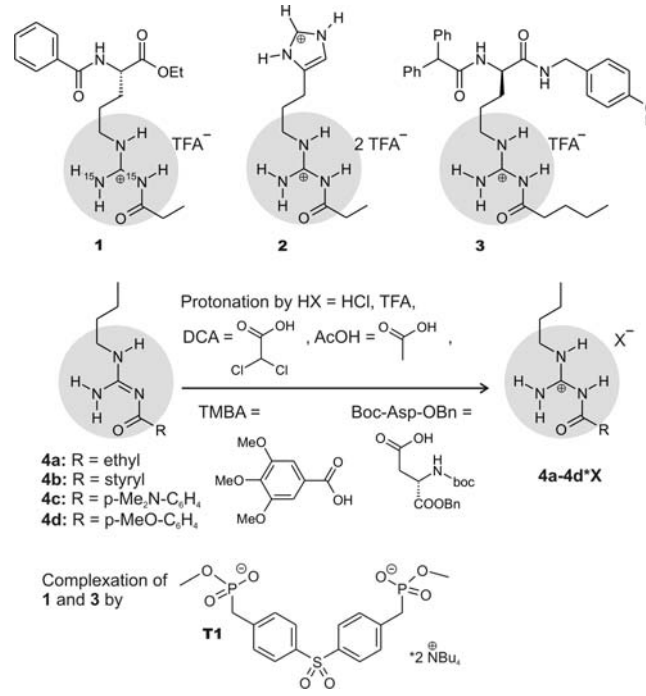

Figure 3. Compounds investigated in this work: [$^{15}N^{\eta}_2$]-Bz-Arg-(N$^{\eta}$-propionyl)-OEt (**1**), *N*-propionyl-*N*′-(3-imidazol-4-ylpropyl)guanidine (**2**), UR-MK50 (**3**), the simple *n*-butyl chain analogues *N*-propionyl-*N*′-butylguanidine (**4a**) and *N*-cinnamoyl-*N*′-butylguanidine (**4b**), and benzoic acid derivatives *N*-*p*-dimethylaminobenzoyl-*N*′-butylguanidine (**4c**) and *N*-*p*-methoxybenzoyl-*N*′-butylguanidine (**4d**). The free bases **4a**−**d** were protonated with one or several of the acids shown to give the 1:1 salts **4a**−**d**·X.

NMR Studies of Protonated Acylguanidines in Solution. Conformational Equilibria and Conformational Assignment. Organic solvents were chosen for all NMR investigations of acylguanidines, because recently Limbach et al. showed that the hydrophobic environment of the active site in the interior of an enzyme, i.e., in the absence of bulk water, may be modeled better by an aprotic solvent than by water.[39] In addition, these solvents strengthen the H-bonds and allow for low-temperature measurements to detect conformational equilibria.

To optimize the NMR investigations of protonated monoalkylated acylguanidines and to identify dynamic equilibria between the different possible conformations, first a screening of the

(36) Igel, P.; Schneider, E.; Schnell, D.; Elz, S.; Seifert, R.; Buschauer, A. *J. Med. Chem.* **2009**, *52*, 2623–2627.
(37) Rudolf, K.; Eberlein, W.; Engel, W.; Wieland, H. A.; Willim, K. D.; Entzeroth, M.; Wienen, W.; Beck-Sickinger, A. G.; Doods, H. N. *Eur. J. Pharmacol.* **1994**, *271*, R11–R13.
(38) Kleinmaier, R.; Gschwind, R. M. *J. Label. Compd. Radiopharm.* **2009**, *52*, 29–32.
(39) Sharif, S.; Fogle, E.; Toney, M. D.; Denisov, G. S.; Shenderovich, I.; Buntkowsky, G.; Tolstoy, P. M.; Huot, M. C.; Limbach, H.-H. *J. Am. Chem. Soc.* **2007**, *129*, 9558–9559.

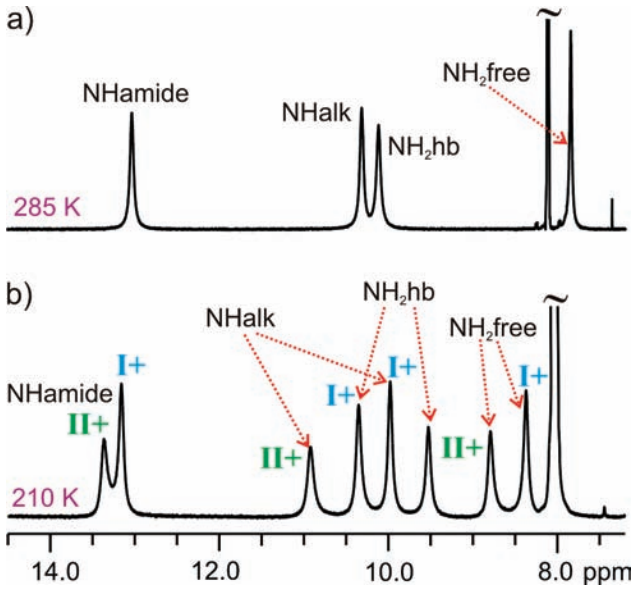

Figure 4. Generally observed dynamic behavior of protonated acylguanidines for the example of **4d**·DCA in CD_2Cl_2/DMSO-d_6 (9:1): (a) at 285 K four NH signals are observed; (b) upon cooling to 210 K the four signals split into eight NH signals, indicating the two conformations I^+ and II^+, which exchange fast on the NMR time scale at elevated temperatures (for labeling see Figure 5).

spectroscopic properties of **1**−**3**·TFA, **4b**·X (X = HCl, TFA, DCA, AcOH, Boc-Asp-OBn, TMBA), **4a**·X, (X = HCl, TFA, DCA, AcOH), **4c**·X (X = TFA, Boc-Asp-OBn), and **4d**·X (X = HCl, TFA, DCA, Boc-Asp-OBn) was performed in a temperature range between 300 and 200 K in CD_2Cl_2/DMSO-d_6 (9:1). This survey revealed, for all protonated monoalkylated acylguanidines in this solvent mixture, one general ^{1}H signal pattern with a similar temperature-dependent behavior, which is shown for the example of **4d**·DCA in Figure 4. At elevated temperatures, four NH signals are detected, which fit perfectly to the four NH protons expected for the acylguanidine moiety (Figure 4a). However, upon cooling these NH signals broaden, show coalescence effects, and split into eight NH resonances, indicating two conformations at low temperatures (Figure 4b). These two conformations, separable at low temperature, are denoted as I^+ and II^+ in Figure 4b and exchange fast on the NMR time scale at elevated temperature (Figure 4a). This general ^{1}H pattern and this trend in the temperature dependence were found for all protonated acylguanidines investigated in this study in this solvent mixture. The individual coalescence temperatures, conformational ratios, and absolute chemical shift values of each complex, however, show slight variations and depend on the anion, microsolvation, and substitution pattern applied (see discussion below).

In the case of several protonated acylguanidines, which show not only well-separated NH signals but also small line widths at low temperatures, the two conformations I^+ and II^+ could be unambiguously assigned as described elsewhere.[40] Generally ^{1}H,^{1}H COSY and ^{1}H,^{13}C HMBC spectra allow the identification of NH_{alk} and NH_{amide} (for labeling see Figure 5). In addition, differentiation among conformations I^+, II^+, and III^+ (see Figure 1) is possible using the spatial information of so-called *w*-couplings within the acylguanidine moiety. These long-range $^4J_{H,H}$ scalar couplings are only detectable in a zigzag arrangement of two NH protons (see marking in Figures 1 and 5) and therefore allow the identification of the spatial arrangement of pairs of NH protons, resulting in the assignment of the two conformations I^+ and II^+. This is exemplarily shown on the NH section of a ^{1}H,^{1}H COSY spectrum of **4b**·TMBA at 200 K in Figure 5. For the major conformation, two *w*-couplings are detected, one to the NH_{amide} (W3) and one to the NH_{alk} (W2). This combination of *w*-couplings allows identification of the major conformation as II^+. For the minor conformation only one *w*-coupling to NH_{alk} (W1) is detected, which allows assignment of this conformation to I^+. These assignments are also in accordance with the relative chemical shifts of the NH resonances, which are influenced by the formation of strong H-bonds to the anion (see below).

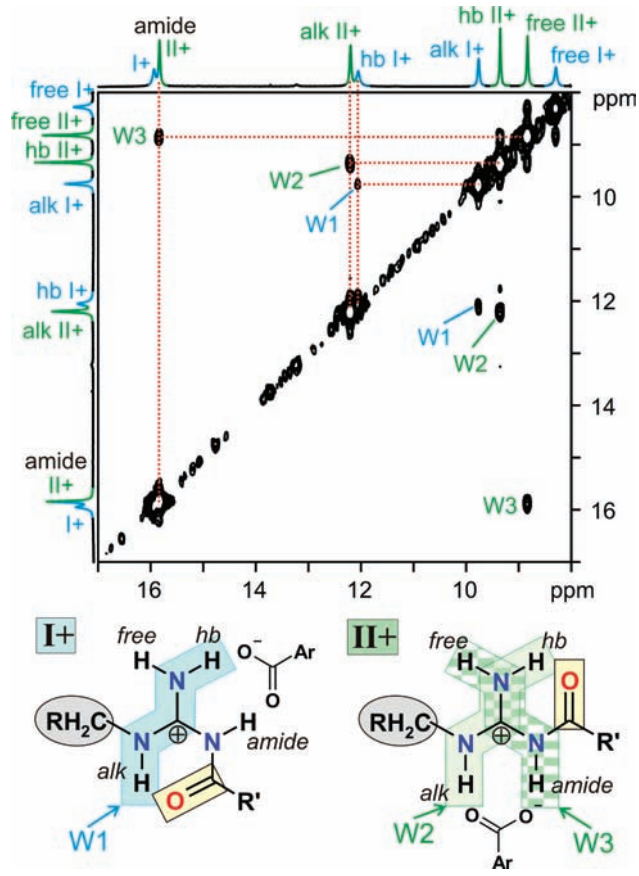

Figure 5. NH section of a ^{1}H,^{1}H COSY spectrum of **4b**·TMBA in CD_2Cl_2 and DMSO-d_6 (9:1) at 200 K. For the major conformation, the detection of the two $^4J_{H,H}$ long-range couplings W2 and W3 allow the assignment to II^+; for the minor conformation, W1 allows the identification of I^+.

Interaction with Anions: A Conformational Exchange Brake. To investigate the influence of the anions on the exchange dynamics between the two conformations of protonated acylguanidines, **4b** in CD_2Cl_2 and DMSO-d_6 (9:1) was selected, because the NMR survey showed for this combination the best-resolved spectra within a wide range of anions. With strong acids, four sharp guanidinium NH signals are detected for **4b** at elevated temperatures, indicating fast exchange between the two conformations on the NMR time scale. This is shown in Figure 6a for the ^{1}H spectrum of **4b**·TFA at 300 K. In addition, the conformational exchange of **4b**·TFA is so fast that the coalescence point is even lower than 210 K (see Figure 6b). In contrast, for **4b**·AcOH, the ^{1}H spectra of the acylguanidine moieties change drastically. At 300 K, only broad signals are detected, which are close to the coalescence point (Figure 6c),

(40) Kleinmaier, R.; Gschwind, R. M. *Magn. Reson. Chem.* **2010**, in press (published online Jul 18, doi: 10.1002/mrc.2648).

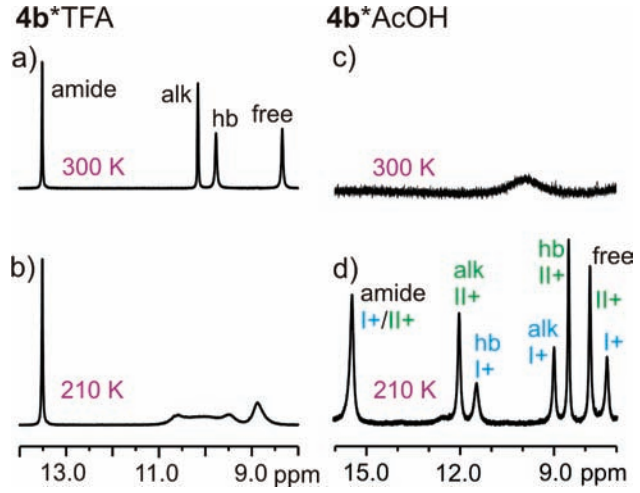

Figure 6. NH sections of the ^{1}H NMR (600 MHz) spectra of **4b**·TFA (a,b) and **4b**·AcOH (c,d) in CD_2Cl_2 and DMSO-d_6 (9:1) at 300 K (a,c) and at 210 K (b,d). The conformational exchange is significantly faster with TFA than with AcOH.

whereas at 210 K, the signals sharpen and the typical chemical shift pattern of the conformations I^+ and II^+ is observed (Figure 6d).

These spectra suggest that the exchange rate between the two conformations can be gradually adjusted by the strength of the interaction with the anion. Therefore, salts of **4b** derived from six different acids (HCl, TFA, DCA, AcOH, Boc-Asp-OBn, and TMBA) were investigated at 210 K, and their ^{1}H spectra are shown in Figure 7, ordered by decreasing acidity. With Cl^- as anion, only one broad and unresolved ^{1}H signal is detected for all six amine protons of both conformations, indicating medium-fast exchange above the coalescence point. With decreasing acidity, i.e., increasing H-bond acceptor strength, the NH signal dispersion becomes better while the resonances are still broad until six separate and rather sharp signals are detected. This indicates reduced conformational exchange with increasing interaction strength between the cationic acylguanidine and its anion.[41] In addition, the signals with the highest chemical shift, the NH_{amide} signals of II^+ and I^+, $NH_{alk}(II^+)$, and $NH_{hb}(I^+)$, experience a strong further increase in chemical shift with decreasing acidity of the acid, whereas the chemical shifts of the remaining NH signals are nearly unaffected by the change of the anion. These selective low-field shifts in the chemical shift pattern can be attributed to the formation of strong H-bonds to the anion,[42] and thus the main positions of the anions in conformations I^+ and II^+ are derived as depicted in Figure 5.[43]

Both the reduced chemical exchange and the higher chemical shift dispersion of specific NH protons indicate specific intermolecular H-bonds to the anion. In addition, the conformational exchange rate is modulated by the H-bond strength.[44,45] It can be seen in Figure 7 that the higher the H-bond acceptor strength, the stronger are the H-bonds between anion and cation and the lower is the conformational exchange rate. Thus, a strong interaction with the anion acts like a brake for the conformational exchange.

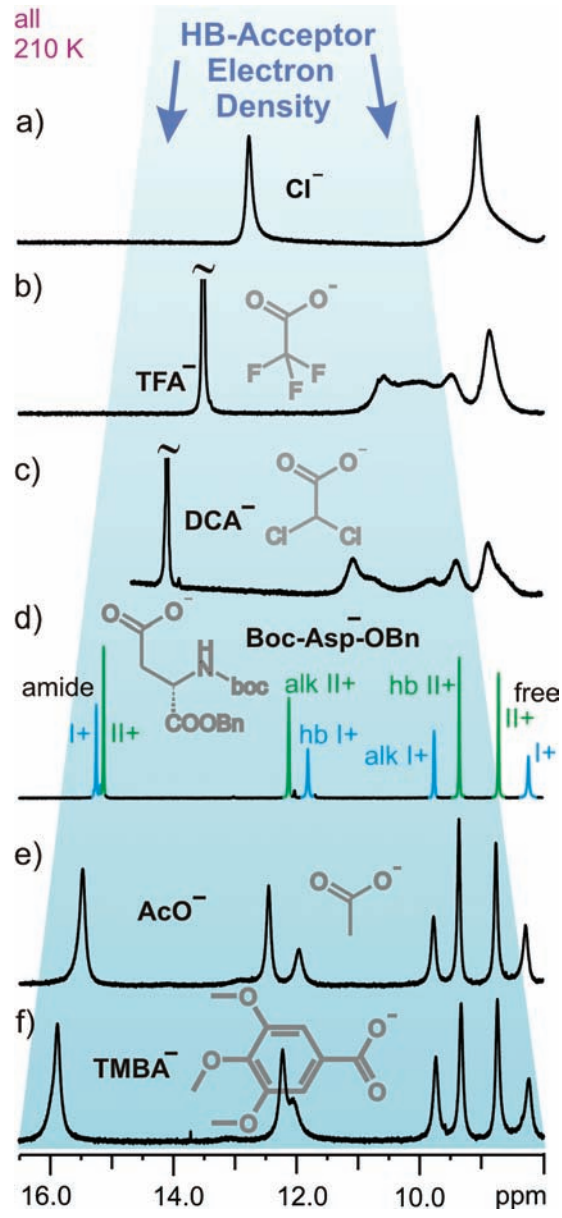

Figure 7. Modulation of the conformational exchange rate and the NH signal dispersion by the H-bond acceptor properties of the anion. Shown are the stacked NH sections of ^{1}H spectra of **4b** in CD_2Cl_2 and DMSO-d_6 (9:1) at 210 K, protonated with six different acids whose anions possess increasing electron densities in the carboxylate, going from lowest at the top (a) to highest at the bottom (f). The exchange rate is reduced and the signal separation is enhanced with reduced acid strength.

(41) Simulations of the conformational exchange rates between I^+ and II^+ for **4b**·Boc-Asp-OBn and **4b**·TFA showed that the broadening of the signals in Figure 7 is dominated by the exchange rate and that the different chemical shift dispersions affect the exchange rates only marginally. According to these simulations, at 210 K the rate constant for the conformational exchange is increased by a factor of 30 when going from the strong H-bond acceptor Boc-Asp-OBn to the much weaker TFA as anions.

(42) Sharif, S.; Denisov, G. S.; Toney, M. D.; Limbach, H.-H. *J. Am. Chem. Soc.* **2007**, *129*, 6313–6327, and references therein.

(43) DOSY spectra of **4a**·DCA at 300 K and **4d**·DCA at 270 K showed identical diffusion coefficients for the anion and the cation. Due to the fast exchange of the NH protons in acylguanidines, the positions of the anions could not be verified by NOESY cross peaks.

(44) We correlate here the H-bond acceptor strength of the anion with the electron density available for H-bonding in the carboxylate moiety, which is typically higher for more basic anions, i.e., when they are derived from weaker acids. This concept of ordering the anions by their electron densities has been checked and confirmed by an analysis of the ^{13}C chemical shifts of the carboxylic carbons of alkali salts of the acids used here (see Supporting Information).

(45) Gojło, E.; Smiechowski, M.; Panuszko, A.; Stangret, J. *J. Phys. Chem. B* **2009**, *113*, 8128–8136.

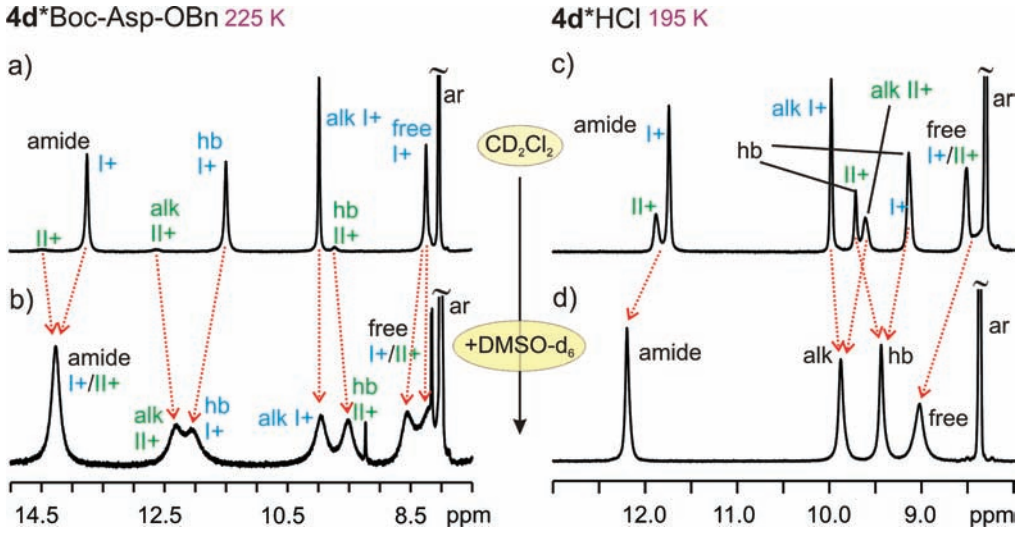

Figure 8. Effect of microsolvation by DMSO on the conformational distribution and exchange rate of protonated acylguanidines. The conformational shift from I^+ to II^+ upon microsolvation by DMSO is shown on the ^1H sections of **4d**·Boc-Asp-OBn at 225 K: (a) 95/5% I^+/II^+ in pure CD_2Cl_2 and (b) 50/50% I^+/II^+ after addition of 10% DMSO-d_6. The acceleration of conformational exchange upon microsolvation by DMSO is demonstrated on the ^1H sections of **4d**·HCl at 195 K: (c) in pure CD_2Cl_2, both conformations are detected (70/30% I^+/II^+), whereas (d) after addition of 3% DMSO-d_6, one conformationally averaged set of signals is observed.

Microsolvation by DMSO. Because of severe solubility problems of protonated monoalkylated acylguanidines in apolar solvents, so far exclusively solvent mixtures (CD_2Cl_2 and DMSO-d_6, 9:1) have been used. In terms of H-bond networks, microsolvation by DMSO means a considerable H-bond acceptor competition between the DMSO solvent molecules and the anion. Additionally, the electrostatic attraction between the anion and the acylguanidinium cation is weakened by the high susceptibility of DMSO. Therefore, the interaction between anion and acylguanidinium cation should be considerably stronger in solvents with reduced susceptibility and without H-bond acceptor properties, such as pure CD_2Cl_2. The compound pool was screened for solubility in pure CD_2Cl_2, and **4d**·Boc-Asp-OBn, **4d**·HCl, and **4c**·Boc-Asp-OBn were found to be sufficiently soluble in pure CD_2Cl_2 to conduct DMSO-d_6 titration experiments at 225 and 195 K, i.e., temperatures at which the conformational exchange is slow on the NMR time scale. Starting from pure CD_2Cl_2, increasing amounts of DMSO were added and the spectral changes monitored, as shown for **4d**·Boc-Asp-OBn and **4d**·HCl in Figure 8. The spectra of **4d**·Boc-Asp-OBn (Figure 8a,b) show impressively that microsolvation with DMSO not only affects the conformational exchange rate, as expected from the results about the interaction with the anions (see above), but also shifts drastically the ratio of the two conformations. In pure CD_2Cl_2, conformation I^+ is strongly predominant over conformation II^+, with a ratio of 95:5 (Figure 8a). However, upon addition of about 10% DMSO-d_6, the portion of the conformation II^+ grows to 50% (Figure 8b). Further addition of DMSO changes the conformational distribution only marginally but leads to significant line broadening, indicating increased conformational exchange (data not shown). Interestingly, the conformational preference for I^+ over II^+ (70:30) is significantly smaller for **4d**·HCl (see Figure 8c), and already addition of less than 5% DMSO (see Figure 8d) leads to one set of four NH signals, i.e., fast exchange between the two conformations on the NMR time scale.

The described trend in the conformational preferences depending on the amount of microsolvation with DMSO and the anion properties now fit perfectly to the interactions with the anions discussed above. For the combination with the strongest H-bond interaction between acylguanidinium moiety and anion, i.e., with a strong H-bond acceptor (Boc-Asp-OBn) and without competing DMSO molecules, the highest preference for conformation I^+ is observed. Upon weakening this interaction either through microsolvation by DMSO or through changing the anion properties, i.e., by replacing Boc-Asp-OBn with Cl^-, the conformational preference for I^+ is significantly reduced. By further weakening the interaction with the anion, e.g., by raising the percentage of DMSO, the exchange between the two conformations becomes too fast to be observed by NMR.

As a result, all data hint at a conformational preference of I^+ induced by a strong interaction with the anion. However, for both conformations, forklike H-bonds to two guanidinium protons are proposed and confirmed by the chemical shift patterns of I^+ and II^+ (see Figure 5 and discussion above), and in both conformations, three NH protons are involved in H-bonds. Thus, at first glance the interaction patterns look quite similar. However, in I^+ the NH_2 group is involved in the intermolecular H-bond, whereas in II^+ the NH_2 group is involved in the intramolecular H-bond. Therefore, we suggest an entropic contribution from the rotation of the NH_2 group inside the H-bond network as the reason for the preference of conformation I^+ in pure CD_2Cl_2. In a partially flexible salt bridge to the anion, the rotational barrier of the NH_2 group is expected to be lower than in an intramolecular H-bond to the carbonyl within a rather rigid six-membered ring. In pure CD_2Cl_2, these H-bonds are strong enough to produce a sufficient difference in total energy, which makes I^+ the preferred conformation. (For a further reasoning and spectral evidence for a NH_2 rotation, see Supporting Information.) Additional H-bond acceptors such as DMSO, reduced electrostatic attraction because of higher susceptibility of the solvent, or anions with reduced interaction strength are expected to lead to lower rotational barriers for the NH_2 group in conformation I^+ and thus to a reduced preference for I^+, as observed experimentally.

Impact of Alkyl and Acyl Substituents. The next step was to investigate whether varying substituents on the acylguanidine moiety affect the conformational preferences or exchange rates. First, the influence of different alkyl substituents was investigated. As evident from the compound pool shown in Figure 3,

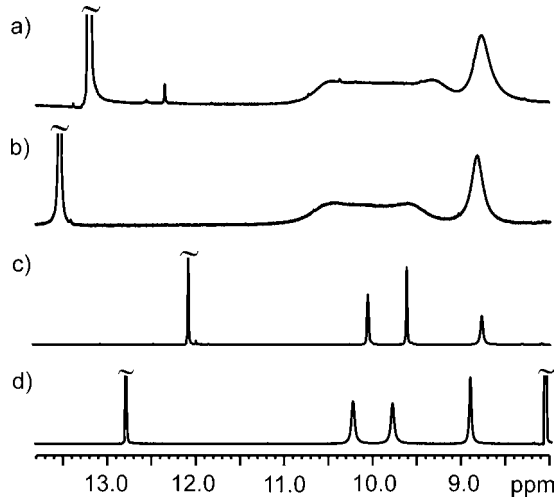

Figure 9. Influence of the electronic properties of the acyl substituent on the strengths of the H-bond network, shown on the ^{1}H sections of (a) **4a**·TFA, (b) **4b**·TFA, (c) **4c**·TFA, and (d) **4d**·TFA at 215 K in CD_2Cl_2 and DMSO-d_6 (9:1). Exchange is much faster, leading to four sharp lines in (c) and (d), because the H-bond network is weakened due to delocalization of the charge.

with **1**, **2**, and **4a**, three different alkyl residues are available with identical acyl moieties. In addition, **3** exhibits only an *n*-butyl instead of an ethyl group in the acyl part, which is expected to induce only marginal changes. Therefore, **3** was also included in the comparison. All four of these compounds have an alkyl chain directly attached to the guanidine moiety. In addition, two amino acid scaffolds are present in **1** and **3**, as well as an imidazolium moiety with a second positive charge in **2**. Comparisons of the ^{1}H spectra of the TFA salts of **1**, **2**, **3**, and **4a** show astonishingly similar signal patterns of the guanidine NH signals and only a slightly reduced exchange for **4a** (see Supporting Information for spectra). This shows that, for protonated acylguanidines, remote changes in the structure, i.e., the presence of additional functional groups potentially capable of forming additional but weaker H-bonds, do not affect the structural properties of the acylguanidine moiety significantly.

Second, the influence of structural changes in the acyl moiety was investigated on **4a**−**d**, which have identical alkyl group but deviating acyl substituents. The ^{1}H spectra of the NH region of the TFA salts of **4a**−**d** at 215 K are shown in Figure 9. Interestingly, the spectra of **4a** with an ethyl group and **4b** with a styryl group are very similar (see Figure 9a,b), aside from small low-field shifts for **4b**. This indicates the formation of slightly stronger H-bonds in **4b**, supported by the additional π-system, which do not significantly affect the exchange rates. In contrast, for **4c** and **4d**, much higher exchange rates are observed. The TFA salts of **4c** and **4d** (see Figure 9c,d) show only four separate peaks with quite narrow line widths, indicating that conformational exchange is already fast on the NMR time scale. As discussed above, this faster conformational exchange can be slowed down by using lower amounts of DMSO (see Supporting Information for spectra). A possible reason for the increased exchange rate is the reduced strength of the intramolecular H-bond caused by the para-substituted phenyl rings acting as electron donators. Additionally, delocalization of the positive charge of the guanidinium carbon over the π-system may weaken the electrostatic interactions with the anions and thus reduce the salt-bridge character of the intermolecular H-bonds. This trend is also evident from the increased chemical shift when comparing **4c** and **4d**: the *p*-dimethylamino-substituted aromatic ring in **4c** is a better mesomeric electron donator than the *p*-methoxy-substituted one in **4d**. Therefore, in **4c** the positive charge of the guanidine unit may be attenuated more than in **4d**. This makes the acylguanidine unit of **4c** a weaker H-bond donator, which manifests in lower chemical shifts of the NH protons affected by H-bonds.[39] Consequently, the most acidic proton, i.e., NH_{amide}, shows the greatest chemical shift change.

These comparisons show that structural changes in remote parts of the alkyl substituent do not affect the structural properties of the acylguanidine moiety significantly. In contrast, acyl substituents that change the electronic or mesomeric properties of the acylguanidine moiety can change the strength of the H-bond network.

Conformations of the Free Base. In addition to the protonated acylguanidines, the spectral and conformational properties of the free acylguanidine bases were investigated to elucidate the effect of protonation on preferred conformations and conformational exchange. For this purpose, the free bases of **4a**−**d** were synthesized and investigated NMR spectroscopically. In accordance with previous reports that the acylimino tautomer was the preferred conformation of unprotonated acylguanidines,[17,46,47] in our spectra of **4a**−**d**, no hint of protonation of the amide nitrogen was found. Therefore, in Figure 1 and in the following, only conformations of the acylimino tautomer are discussed.

NMR investigations of **4a**−**c** revealed again the existence of two conformations at low temperatures, which show conformational exchange at elevated temperatures and a shift in the conformational preferences upon microsolvation by DMSO. Both effects are exemplarily shown on the ^{1}H spectra of **4d** in Figure 10. Again, the NH_{alk} resonances of both conformations were unambiguously assigned on the basis of ^{1}H,^{1}H COSY cross peaks to the alkyl substituents. Regarding the NH_2 protons, in the spectra of conformation II of **4d**, a $^2J_{NH_2}$ splitting of 4.5 Hz was observed, confirming the assignment. However, in contrast to the protonated acylguanidines, for none of the unprotonated acylguanidines were $^4J_{H,H}$ scalar couplings detected, which was attributed to the reduced delocalization of the double bond. Therefore, the further conformational assignment was based on the interpretation of chemical shift differences and dimerization trends measured by ^{1}H,^{1}H DOSY spectra. Interestingly, for the two sets of NH signals, very similar diffusion coefficients were measured, indicating dimers for both conformations in pure CD_2Cl_2 (for details, see Supporting Information). As evident from Figure 1, conformations I and II exhibit both structurally typical and very similar dimerization sites, with the unprotonated amide nitrogen and one NH proton on the same side. In contrast, conformation III does not possess such an H-bond donor/acceptor pair, and intermolecular interactions with the amide nitrogen are hampered by severe steric hindrance. These structural features of III should lead to a significantly reduced aggregation tendency compared to I and II. Therefore, on the basis of the nearly equal diffusion coefficients of the two observed conformations, conformation III was excluded.

The remaining assignment starts from the two unambiguously assigned NH_{alk} signals. In I, the NH_{alk} proton is in the intramolecular H-bond and will exert the highest chemical shift. This is found for the conformation with the broad line widths (see Figure 10b−d). In contrast, in the second set of signals,

(46) Skawinski, W. J.; Ofsievich, A.; Venanzi, C. A. *Struct. Chem.* **2002**, *13*, 73–80.
(47) Venanzi, C. A.; Plant, C.; Venanzi, T. J. *J. Comput. Chem.* **1991**, *12*, 850–861.

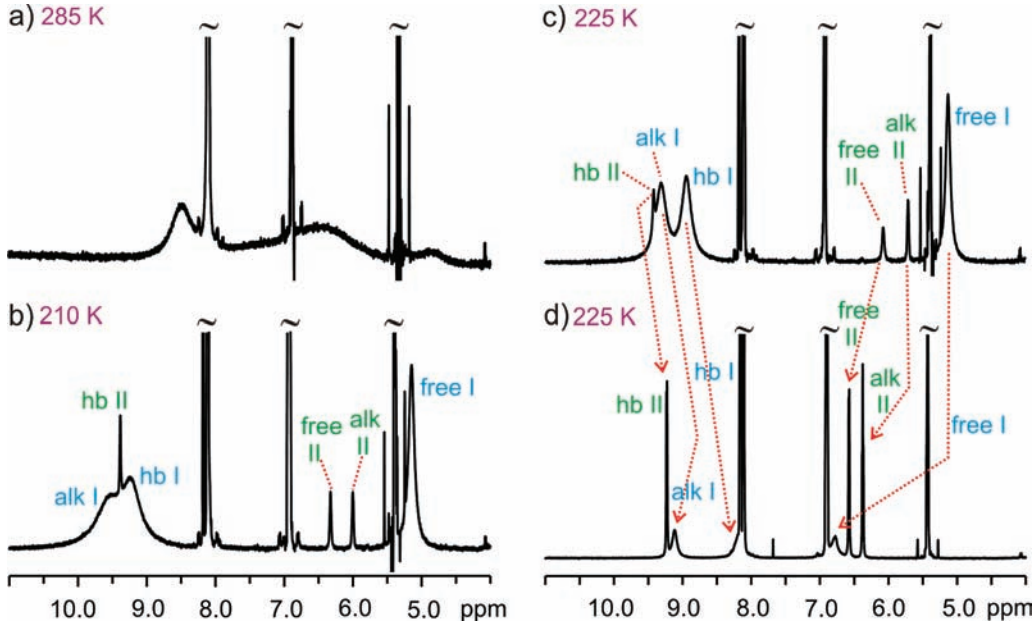

Figure 10. Unprotonated acylguanidines. Again, increased temperature leads to conformational exchange, as shown in the NH sections of the ^{1}H spectra of **4d** in pure CD_2Cl_2 at (a) 285 and (b) 210 K, and again, a conformational shift from I to II upon microsolvation by DMSO is observed, as shown in the ^{1}H spectra of **4d** at 225 K in (c) pure CD_2Cl_2 and (d) CD_2Cl_2 and DMSO-d_6 (9:1).

NH_{alk} has the lowest chemical shift value, in accordance with conformation II. For further interpretations of the line widths and chemical shift patterns of I and II, see the Supporting Information.

The ^{1}H spectra of **4d** in pure CD_2Cl_2 (Figure 10c) and after addition of 10% DMSO (Figure 10d) now reveal that, also in the unprotonated acylguanidines, conformation I is highly preferred (about 93/7% I/II) and that microsolvation with 10% DMSO shifts the preferred conformation to II (about 42/58% I/II). Similar to the protonated acylguanidines, the conformational preference for I in pure CD_2Cl_2 might be driven by intermolecular interactions, which are weakened upon microsolvation by DMSO, allowing the portion of conformation II to grow. In contrast to the protonated acylguanidines, in which the interaction with the anion determines the conformational preference, one can speculate that, in unprotonated acylguanidines, the dimerization properties of the conformations may be crucial for the conformational preference. Besides stronger H-bonds in the dimer of I, which are suggested by the chemical shift pattern and geometry-optimized structure of the dimer (see Supporting Information for details), again the entropic properties seem to promote conformation I in the dimer. This is strongly suggested by the broad line widths of the NH signals in I, indicating conformational flexibility within the dimer, even in pure CD_2Cl_2 (see Figure 10b,c).

Conformational Preferences in More Complex Receptors. With regard to the relevance of acylguanidines as ligands for pharmacologically important receptor proteins, the conformational preferences in a more complex receptor system were studied. One example, recently published by our group,[32] is the additional complexation of **1**·TFA by a bisphosphonate tweezers molecule, which resembles an artificial arginine fork (see Figure 2a). This complex was also measured in CD_2Cl_2/DMSO-d_6 (9:1). Interestingly, the acylguanidine was found to adopt exclusively conformation II^+ at 220 K. The NMR detection of scalar couplings across two H-bonds in combination with the significantly reduced line widths of the NH signals allow us to exclude significant contributions from any chemical exchange or rotational movements within the H-bond network.

In addition, the complex of the NPY Y_1 receptor antagonist **3** with **T1** (see Figure 11) was investigated. This highly biologically active ligand contains various additional functional groups that are expected to form additional H-bonds. The ^{1}H spectra of this complex show one major conformation (~60%) with sharp line widths and one minor conformation with mainly extremely broad NH signals (for spectra and details, see Supporting Information). The major conformation could be assigned to II^+ on the basis of long-range $^4J_{H,H}$ couplings as described above, and four $^{2h}J_{H,P}$ scalar couplings could be detected, indicating intermolecular H-bonds (see Figure 11a and Supporting Information for spectra). For the minor conformation, no structural information could be detected due to the broad line widths. Therefore, it cannot be distinguished whether this minor conformation shows deviations in the acylguanidine conformation or different modes of interaction or conformations in the part of **3** remote from the acylguanidine.

These results seem to suggest that additional strong H-bond acceptors do not reverse the conformational trends described above for the free acylguanidine salts but rather support the preference and stability of conformation II^+ in complex H-bond networks. This trend is also in agreement with a docking study of the histamine H_2 GPCR ligand in the binding pocket of the guinea pig H_2 receptor (see Figure 2c), which results in conformation II^+ for the complex receptor surrounding in the active site of the transmembrane protein.[9]

Conformational Preferences in Crystal Structures. In addition to the NMR studies, further conformational information about monoalkyl-substituted acylguanidines was collected from X-ray structures. Besides the one previously published crystal structure of an unprotonated imidazolylpropylguanidine,[9] which adopts conformation I (see Figure 2a), two further crystal structures were obtained from our compound pool, **4b** and **4d**·HCl (see

(48) *Spartan*; Wavefunction, Inc.: Irvine, CA, 1991−2007.

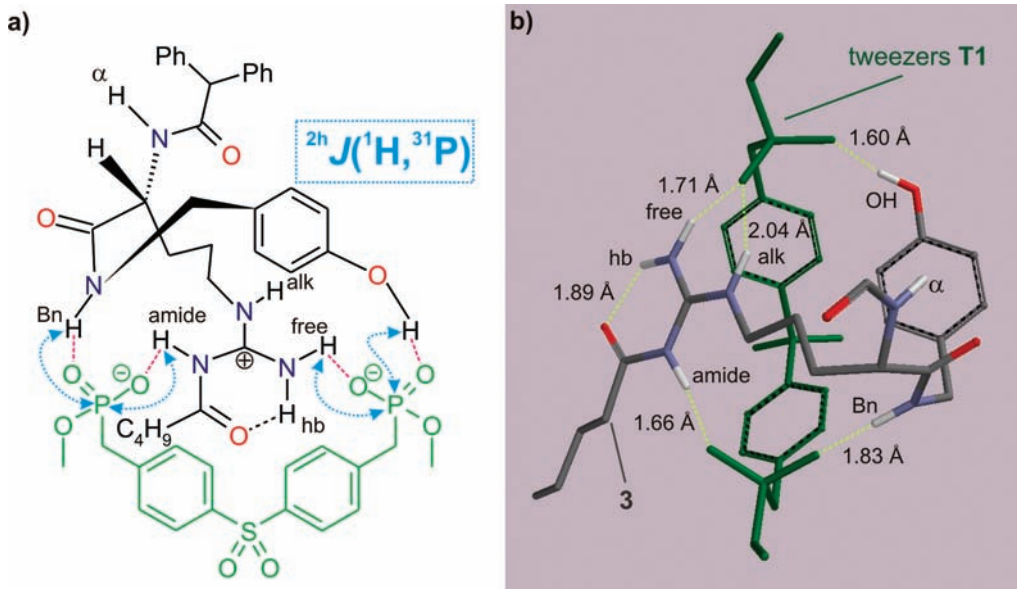

Figure 11. Complex between **3** and bisphosphonate tweezers **T1** (green). (a) Schematic representation adapted to the H-bond pattern observed. $^{2h}J_{H,P}$ scalar couplings (dotted arrows) indicate the experimentally determined intermolecular H-bonds shown by dashed lines (magenta). (b) Geometry-optimized 3D representation showing the four experimentally detected plus one additional intermolecular H-bonds (dashed lines, yellow), with H···O distances as calculated by Spartan[48] (for details, see Supporting Information).

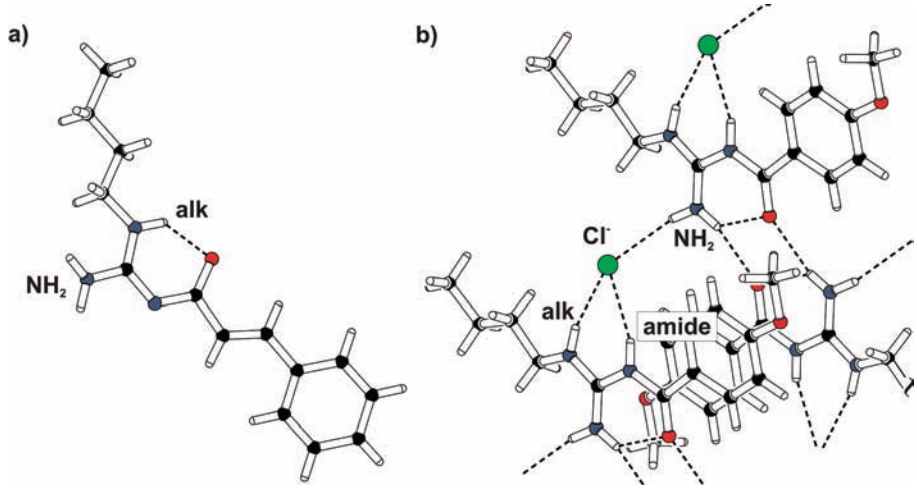

Figure 12. Crystal structures of (a) unprotonated **4b** showing conformation I and (b) **4d**·HCl adopting conformation II$^+$ in a complex H-bond network between antiparallel strands of **4d**·HCl (see text).

Figure 12). All attempts to crystallize further compounds failed, especially those to obtain crystals of carboxylate salts.

In the crystal structure of the unprotonated **4b**, the intramolecular H-bond is found to be highly probable between the NH_{alk} group and the carbonyl oxygen, indicating conformation I (see Figure 12a). Thus, in both crystal structures of monoalkylated acylguanidines known so far, conformation I is observed, which agrees nicely with the major conformation in pure CD_2Cl_2 found in the NMR studies (see Figure 10b,c).

In contrast, the crystal structure of the protonated **4d**·HCl shows conformation II$^+$, with a complex network of H-bonds (see Figure 12b). The chloride is in H-bonding distance (<2.5 Å) to three NH protons and interconnects two parallel planes in the crystal, which are formed by antiparallel strands of **4d**·HCl. These strands themselves are interconnected via H-bonds between two antiparallel acylguanidinium units. Interestingly, the observed conformation II$^+$ is again closely related to the NMR observations. First, the NMR spectra of HCl salts of acylguanidines in pure CD_2Cl_2 contain considerable amounts of conformation II$^+$ (e.g., 30% II$^+$ for **4d**·HCl see Figure 8). Second, the complex H-bond network observed in the crystal structure might resemble the complex H-bonds induced upon DMSO microsolvation in solution and further supports the preference for conformation II$^+$. Thus, the three crystal structures of monoalkylated acylguanidines known so far not only adopt exclusively the conformations found in our NMR studies but in addition resemble the principal conformational preferences observed in solution.

Conclusion

Throughout the whole study of monoalkylated acylguanidines, exclusively two (I/I$^+$ and II/II$^+$) out of eight possible acylguanidine conformations were detected in both the unprotonated state and the protonated state, independent of the compound, the anion, or the solvent used. The intermolecular interactions between the monoalkylated acylguanidines and the anions,

solvent molecules, or biomimetic receptors decide both the conformational preferences and exchange rates. Also, in the presence of receptor molecules forming additional strong H-bonds to protonated acylguanidines, conformation II^+ was found exclusively for two different acylguanidines in NMR studies with bisphosphonate tweezers and also in a previous docking study with a membrane protein. Even the crystal structures of acylguanidines known so far resemble the conformational trend identified in this study.

In summary, this study gives for the first time detailed insight into the conformational preferences of monoalkylated acylguanidines. Considering the potential of these acylguanidines in medicinal chemistry and the fact that, in the past, such known preferences often led to ligands with greatly increased affinity through the rigidization of the ideal binding conformation,[49−51] the presented work may contribute to the prediction and rational design of biologically active compounds containing monoalkylated acylguanidines.

Experimental Section

Routine NMR measurements were conducted on Bruker Avance 300, 400, and 600 MHz spectrometers equipped with 5 mm BBI or TBI probeheads. The variable-temperature experiments were conducted on a Bruker Avance 600 MHz spectrometer equipped with a BVT 3000 variable-temperature unit. Deuterated NMR solvents were purchased from Aldrich, Deutero, and Merck.

Starting materials were obtained from Sigma-Aldrich and Merck. Solvents were distilled prior to use.

For clarity, please refer to the Supporting Information for a synthetic scheme.

(*R*)-N^{α}-(2,2-Diphenylacetyl)-*N*-(4-hydroxybenzyl)-N^{ω}-pentanoylargininamide (3, UR-MK50). Pentanoic anhydride (97.6 mg, 0.52 mmol, 1.1 equiv) was added to a solution of (*R*)-*N*-(4-*tert*-butoxybenzyl)-N^{ω}-*tert*-butoxycarbonyl-N^{α}-(2,2-diphenylacetyl)argininamide (300 mg, 0.48 mmol, 1 equiv) and NEt_3 (48 mg, 66 μL, 0.48 mmol, 1 equiv) in CH_2Cl_2 (10 mL). The mixture was stirred at room temperature (rt) for 5 h. Trifluoroacetic acid (TFA) (10 mL) was added, and stirring was continued at rt for 2 h. MeOH (30 mL) was added, followed by evaporation under reduced pressure. Purification with preparative HPLC (column: Eurospher-100 C18, 250 × 32 mm, 5 μm; Knauer, Berlin, Germany) and lyophilization afforded the product as a white fluffy solid (190 mg, 0.28 mmol, 59%), mp > 118 °C (decomp.). ^{1}H NMR (400 MHz, CD_3OD, COSY): δ (ppm) 0.93 (t, 3H, ^3J = 7.35 Hz, CH_3), 1.37 (m, 2H, C$\underline{H}_2$-CH_3), 1.48−1.76 (bm, 5H, CH-C$\underline{H}_2$-C$\underline{H}_2$, C$\underline{H}_2$-CH_2-CH_3), 1.83 (m, 1H, CH-C$\underline{H}_2$-CH_2), 2.45 (t, 2H, ^3J = 7.44 Hz, CH_2-CO), 3.23 (m, 2H, CH_2-C$\underline{H}_2$-NH), 4.2 (d, 1H, ^2J = 14.6 Hz, C$\underline{H}_2$-ArOH), 4.26 (d, 1H, ^2J = 14.59 Hz, C$\underline{H}_2$-ArOH), 4.43 (m, 1H, CH^{α}), 5.07 (s, 1H, C$\underline{H}$-$(Ph)_2$), 6.7 (d, 2H, ^3J = 8.6 Hz, AA′BB′), 7.04 (d, 2H, ^3J = 8.62 Hz, AA′BB′), 7.16−7.31 (m, 10H, Ph). RP-HPLC (210 nm): 99% (t_R = 16.6 min, k = 5.1). HR-MS (FAB^+, MeOH/glycerin): *m*/*z* calcd for $[C_{32}H_{39}N_5O_4 + H]^+$ 558.3080, found 558.3080; $C_{32}H_{39}N_5O_4 \times C_2HF_3O_2$, 671.7.

***N*-Propionyl-*N*′-butylguanidine (4a).** The preparation of [$^{15}N_2$]-*N*-Boc-*N*′-propionyl-*S*-methylisothiourea has been published elsewhere.[38] According to that protocol, the unlabeled compound *N*-Boc-*N*′-propionyl-*S*-methylisothiourea was prepared and reacted with an excess of butylamine to yield *N*-Boc-*N*′-propionyl-*N*″-butylguanidine, which was Boc-deprotected to obtain **4a**.

***N*-Boc-*N*′-propionyl-*N*″-butylguanidine.** *N*-Boc-*N*′-propionyl-*S*-methylisothiourea (0.35 g, 1.42 mmol) was dissolved in dichloromethane (DCM) (5 mL) at rt, and butylamine (0.69 mL, 7.10 mmol) was added in one batch via syringe. The mixture was stirred for 3 h and then washed once with saturated aqueous $NaHCO_3$ solution, water, and brine, respectively. The organic phase was dried over Na_2SO_4, and the solvents were evaporated under reduced pressure. The colorless oily residue was purified by column chromatography over silica gel to yield pure *N*-Boc-*N*′-propionyl-*N*″-butylguanidine (0.30 g, 78%). ^{1}H NMR (300 MHz, $CDCl_3$, 300 K): δ 0.90 (t, 3H), 1.18 (t, 3H), 1.35 (m, 2H), 1.48 (s, 9H), 1.51 (m, 2H), 2.42 (q, 2H), 3.39 (q, 2H), 8.95 (as, 1H), 12.43 (s, 1H).

***N*-Propionyl-*N*′-butylguanidine (4a). TFA and DCA Salts.** *N*-Boc-*N*′-propionyl-*N*″-butylguanidine was dissolved in dry DCM with 50% TFA or dichloroacetic acid (DCA), respectively, upon cooling with an ice bath and then allowed to warm to rt. After 3 h the solvents were evaporated in vacuo, and the product was purified. The oily residue was subjected to column chromatography over silica gel to yield the pure TFA or DCA salt.

TFA Salt: 0.30 g (1.11 mmol) of starting compound gave 0.21 g of product (80%). ^{1}H NMR (300 MHz, $CDCl_3$, 300 K): δ 0.96 (t, 3H, ^3J = 7.31 Hz), 1.16 (t, 3H, ^3J = 7.49 Hz), 1.42 (m, 2H), 1.65 (m, 2H), 2.55 (q, 2H, ^3J = 7.49 Hz), 3.30 (m, 2H), 7.34 (s, 1H), 9.74 (s, 1H), 9.86 (as, 1H), 13.07 (s, 1H).

DCA Salt: 0.09 g (0.33 mmol) of starting compound gave 0.05 g of product (50%). ^{1}H NMR (300 Hz, $CDCl_3$, 300 K): δ 0.96 (t, 3H, ^3J = 7.31 Hz), 1.16 (t, 3H, ^3J = 7.49 Hz), 1.43 (m, 2H), 1.67 (m, 2H), 2.55 (q, 2H), 3.38 (m, 2H), 5.89 (s, 1H, DCA), 7.30 (s, 1H), 9.82 (s, 1H), 10.06 (s, 1H), 13.40 (s, 1H).

Liberation of Free Base of 4a. *N*-Boc-*N*′-propionyl-*N*″-butylguanidine (0.10 mg, 0.37 mmol) was deprotected with 50% TFA in dry DCM. The crude product (oily residue) was subjected to column chromatography over silica gel in the presence of 5% triethylamine (TEA) to yield the pure free base after evaporation of solvents (0.05 g, 78%). ^{1}H NMR (300 MHz, $CDCl_3$, 300 K): δ 0.89 (t, 3H, ^3J = 7.31 Hz), 1.06 (t, 3H, ^3J = 7.49 Hz), 1.37 (m, 2H), 1.55 (m, 2H), 2.23 (q, 2H, ^3J = 7.49 Hz), 3.10 (m, 2H). ^{13}C NMR: δ 10.0, 13.6, 20.0, 30.8, 33.4, 40.8, 161.1, 186.9. HR-MS (EI): *m*/*z* calcd 171.1372, found 171.1369.

HCl Salt. The free base was treated with a mixture of 10% concentrated aqeuous HCl and 90% MeCN at rt and stirred for 5 min. The solvents were evaporated to yield the colorless solid product quantitatively. ^{1}H NMR (600 MHz, CD_2Cl_2/10% $(CD_3)_2SO$, 285 K, ref TMS internal): δ 0.95 (t, 3H, ^3J = 7.31 Hz), 1.16 (t, 3H, ^3J = 7.49 Hz), 1.42 (m, 2H), 1.62 (m, 2H), 2.53 (q, 2H, ^3J = 7.49 Hz), 3.29 (m, 2H), 8.66 (s, 1H), 8.80 (s, 1H), 9.27 (as, 1H), 12.58 (s, 1H). For complete ^{13}C data (assignment via HSQC, HMBC), see Supporting Information.

AcOH Salt. Prepared in situ by titration of the free base with AcOH, both dissolved in the required NMR solvent, until integration proved a 1:1 ratio. For spectral data, see Supporting Information.

***N*-Cinnamoyl-*N*′-butylguanidine (4b). 1*H*-Pyrazol-1-carboxamidine Hydrochloride.** Aminoguanidinium hydrogen carbonate (13.60 g, 100 mmol) was dissolved in water (25 mL) upon addition of concentrated HCl (17 mL). To the resulting clear solution was added 1,1,3,3-tetramethoxypropane (17.29 mL, 105 mmol) over 15 min using a dropping funnel. The mixture was warmed to 45 °C and stirred for 3 h at that temperature. Evaporation of the solvent to the beginning of crystallization and completion upon resting in the refrigerator yielded large colorless crystals of 1*H*-pyrazol-1-carboxamidine hydrochloride, which were suctioned off to obtain the clean product. Yield: 10.3 g, 70.3 mmol, 70.3%. ^{1}H NMR (300 MHz, CD_3OD, 300 K): δ 6.75 (dd, 1H, ^3J = 1.45 Hz, ^3J = 3.05 Hz, pyrazol-4-H), 7.98 (d, 1H, ^3J = 1.45 Hz, pyrazol-H), 8.48 (d, 1H, ^3J = 3.05 Hz, pyrazol-H).

***N*-Cinnamoyl-1*H*-pyrazol-1-carboxamidine.** 1*H*-Pyrazol-1-carboxamidine hydrochloride (1.00 g, 6.84 mmol) was dissolved in DCM (15 mL), and TEA (1.94 mL, 13.68 mmol) was added. Cinnamoyl chloride (1.14 g, 6.84 mmol) dissolved in DCM (10 mL) was added upon cooling in an ice bath through a dropping funnel. After 3 h of stirring, the mixture was washed once with

(49) Boeckler, F.; Gmeiner, P. *Pharmacol. Therapeut.* **2006**, *112*, 281–333.
(50) Boeckler, F.; Gmeiner, P. *Biochim. Biophys. Acta* **2007**, *1768*, 871–887.
(51) Kubinyi, H. *Pharm. Acta Helv.* **1995**, *69*, 259–269.

saturated aqueous $NaHCO_3$ solution, water, and brine, respectively. The organic phase was dried over Na_2SO_4 and the solvent evaporated under reduced pressure. Column chromatography in DCM over silica gel ($R_f = 0.5$) was necessary to isolate the pure product (0.90 g, 55%). ^{1}H NMR (400 MHz, $CDCl_3$, 300 K): δ 6.46 (dd, 1H, $^3J = 1.59$ Hz, $^3J = 2.76$ Hz), 6.75 (d, 1H, $^3J = 15.91$ Hz), 7.32−7.43 (m, 3H, Ph), 7.55−7.63 (m, 2H, Ph), 7.72 (1H pyrazol +1H NH), 7.85 (d, 1H, $^3J = 15.91$ Hz), 8.57 (d, 1H, $^3J = 2.76$ Hz), 10.00 (bs, 1H, NH).

***N*-Cinnamoyl-*N′*-butylguanidine (4b).** *N*-Cinnamoyl-1*H*-pyrazol-1-carboxamidine (0.50 g, 2.08 mmol) was dissolved in DCM (5 mL), and TEA (0.29 mL, 2.08 mmol) was added. Butylamine (1.05 mL, 10.4 mmol) was added via syringe and the mixture stirred at rt for 1 h. The solvents were evaporated, the oily residue was taken up in ethyl acetate, and petroleum ether was added. Upon resting in the refrigerator, the clean product precipitated (0.31 g, 61%). Recrystallization following the same procedure yielded crystals of **4b** suitable for X-ray crystallography. ^{1}H NMR (600 MHz, $CDCl_3$, 300 K): δ 0.96 (t, 3H, $^3J = 7.42$ Hz), 1.44 (m, 2H), 1.64 (m, 2H), 3.18 (m, 2H), 6.60 (d, 1H, $^3J = 15.91$ Hz), 7.28−7.38 (m, 3H, Ph), 7.62 (d, 1H, $^3J = 15.91$ Hz). HR-MS (EI): *m*/*z* calcd 245.1528, found 245.1534.

Preparation of Salts. HCl Salt. The free base was treated with a mixture of 10% concentrated aqueous HCl and 90% MeCN at rt and stirred for 5 min. The solvents were evaporated to yield the colorless solid product quantitatively. For complete ^{1}H and ^{13}C data (assignment via HSQC, HMBC), see Supporting Information.

TFA Salt. The free base was treated with 5% TFA in MeCN at rt and stirred for 5 min. The solvents were evaporated to yield the colorless solid product quantitatively.

Salts with DCA and AcOH. The free base was titrated in situ with a carboxylic acid, both dissolved in the required NMR solvent, until integration proved a 1:1 ratio. For spectral data, see Supporting Information.

Salts with Boc-L-Asp-OBn and 3,4,5-Trimethoxybenzoic Acid. The free base and the respective acid were weighed to 1:1 stoichiometry and dissolved in the required NMR solvent. For spectral data, see Supporting Information.

***N*-*p*-Dimethylaminobenzoyl-*N′*-butylguanidine (4c). *N*-*p*-Dimethylaminobenzoyl-1*H*-pyrazol-1-carboxamidine.** *p*-Dimethylaminobenzoyl chloride was prepared by refluxing *p*-dimethylaminobenzoic acid (2 g, 12.1 mmol) in 15 mL of $CHCl_3$ with 0.5 mL of dimethylformamide and thionyl chloride (1.73 g, 14.5 mmol) for 1 h. This reaction solution was added in one batch to a solution of 1*H*-pyrazol-1-carboxamidine hydrochloride (2.13 g, 14.5 mmol) in $CHCl_3$ (15 mL) and TEA (8.4 mL, 60.5 mmol) while cooling with an ice bath. The mixture was allowed to warm to rt, stirred for 2 h, and then washed once with saturated aqueous $NaHCO_3$ solution, water, and brine, respectively. The organic phase was dried over Na_2SO_4 and the solvent evaporated under reduced pressure. The product crystallized from $CHCl_3$ pure enough for the next step (2.90 g, 93%). ^{1}H NMR (300 MHz, $CDCl_3$, 300 K): δ 3.06 (s, 3H, -NMe_2), 6.46 (dd, 1H, $^3J = 1.59$ Hz, $^3J = 2.76$ Hz), 6.69 (m, 2H), 7.5−7.75 (s, 1H pyrazol + bs, 1H NH), 8.20 (m, 2H), 8.63 (d, 1H, 2.76 Hz), 10.04 (bs, 1H, NH).

***N*-*p*-Dimethylaminobenzoyl-*N′*-butylguanidine (4c).** *N*-*p*-Dimethylaminobenzoyl-1*H*-pyrazol-1-carboxamidine (1.0 g, 3.89 mmol) was dissolved in $CHCl_3$ (5 mL), butylamine (1.90 mL, 19.5 mmol) was added via syringe, and the mixture was stirred at rt for 1 h. Since TLC analysis showed no conversion, the reaction mixture was heated under refluxing conditions for 3 h. The solvents were evaporated, and a solution of the oily product mixture in diethyl ether was prepared, from which the pure product was precipitated as the sulfate salt by addition of 1 M aqueous H_2SO_4. The free base was liberated by addition of 1 M aqueous NaOH to the crystalline salt covered by ethyl acetate. After phase separation, the pure free base was obtained by evaporation of the solvent. ^{1}H NMR (600 MHz, CD_2Cl_2, 300 K): δ 0.95 (t, 3H, $^3J = 7.35$ Hz), 1.42 (m, 2H), 1.61 (m, 2H), 2.99 (s, 3H, -NMe_2), 3.20 (bs, 2H), 6.65 (m, 2H, ar), 8.01 (m, 2H, ar). HR-MS (EI): *m*/*z* calcd 262.1794, found 262.1789.

***N*-*p*-Methoxybenzoyl-*N′*-butylguanidine (4d). *N*-*p*-Methoxybenzoyl-1*H*-pyrazol-1-carboxamidine.** 1*H*-Pyrazol-1-carboxamidine hydrochloride (1.00 g, 6.84 mmol) was dissolved in $CHCl_3$ (15 mL), and TEA (1.94 mL, 13.68 mmol) was added. p-Methoxybenzoyl chloride (1.14 g, 7.52 mmol) dissolved in $CHCl_3$ (5 mL) was added upon cooling in an ice bath through a dropping funnel. The mixture was allowed to warm to rt, stirred for 2 h, and then washed once with saturated aqueous $NaHCO_3$ solution, water, and brine, respectively. The organic phase was dried over Na_2SO_4 and the solvent evaporated under reduced pressure. Column chromatography in ethyl acetate/petroleum ether (2:5) over silica gel ($R_f = 0.5$) was necessary to isolate the pure product (1.50 g, 90%). ^{1}H NMR (300 MHz, $CDCl_3$, 300 K): δ 3.88 (s, 3H, -OMe), 6.49 (dd, 1H, $^3J = 1.59$ Hz, $^3J = 2.76$ Hz), 6.95 (m, 2H), 7.75 (1H pyrazol + 1H NH), 8.26 (m, 2H), 8.65 (as, 1H), 10.08 (bs, 1H, NH).

***N*-*p*-Methoxybenzoyl-*N′*-butylguanidine (4d).** *N*-*p*-Methoxybenzoyl-1*H*-pyrazol-1-carboxamidine (0.75 g, 3.07 mmol) was dissolved in $CHCl_3$ (5 mL), butylamine (1.56 mL, 15.4 mmol) was added via syringe, and the mixture was stirred at rt for 1 h. The solvents were evaporated, and crude column chromatography in ethyl acetate/petroleum ether yielded the crude product with pyrazol impurity. The pure HCl salt crystallized after addition of 1 M aqueous HCl to a solution of the oily product mixture in diethyl ether. This yielded crystals of the HCl salt suitable for X-ray crystallography. The free base was liberated from the crystalline salt by dissolution in $CHCl_3$ and addition of 1 M aqueous NaOH. Characterization data are given for the HCl salt. ^{1}H NMR (600 MHz, $CDCl_3$, 300 K): δ 0.97 (t, 3H, $^3J = 7.42$ Hz), 1.49 (m, 2H), 1.73 (m, 2H), 3.48 (m, 2H), 3.86 (s, 3H, -OMe), 6.99 (m, 2H, ar), 7.77 (s, 1H, NH), 8.29 (m, 2H, ar), 9.53 (s, 1H, NH), 10.03 (s, 1H, NH), 11.89 (s, 1H, NH). HR-MS (EI): *m*/*z* calcd 249.1477, found 249.1476.

Computational Details. Equilibrium geometry calculations at ground state were carried out by means of the Spartan '06[48] program package using the standard Hartree−Fock 3-21G basis set.

Acknowledgment. This work was supported by the Graduiertenkolleg GRK 760 "Medicinal Chemistry: Molecular Recognition − Ligand-Receptor Interactions" of the DFG. We thank Dr. S. Joseph for invaluable aid in the graphical representation of the X-ray structures.

Supporting Information Available: Spectra, complete ref 4, crystallographic data (.cif) files for **4b** (CCDC 772555) and **4d·HCl** (CCDC 772556), as well as synthetic and computational details. This material is available free of charge via the Internet at http://pubs.acs.org.

JA103756Y